CHARLES UNIVERSITY

FACULTY OF PHARMACY IN HRADEC KRÁLOVÉ

DIPLOMA THESIS

Synthesis of anionic phthalocyanines

Jorge Lozano Cañadilla

Supervisor: Prof. PharmDr. Petr Zimčík Ph.D.

2024

ABSTRACT

Charles University, Faculty of Pharmacy in Hradec Králové
Department of Pharmaceutical Chemistry and Pharmaceutical Analysis
Candidate: Jorge Lozano Cañadilla
Supervisor: prof. PharmDr. Petr Zimčík, Ph.D.
Topic: Synthesis of anionic phthalocyanines

This diploma thesis focuses on the synthesis of anionic phthalocyanines with carboxylic groups for potential use in photodynamic therapy (PDT). The study outlines the importance of water solubility in photosensitizer design for effective PDT.

The synthesis process involved various reactions, including esterification, Suzuki-Miyaura cross-coupling, and cyclotetramerization, to create water-soluble compounds.

The experimental section details the steps taken to obtain the final products, highlighting the challenges faced, such as experimental errors and separation difficulties.

The results and discussion section analyzes the outcomes, emphasizing the significance of specific reaction conditions and purification techniques.

Overall, this work contributes to the development of anionic phthalocyanines with improved properties for PDT, aiming to enhance their efficacy.

ABSTRACT

Univerzita Karlova, Farmaceutická fakulta v Hradci Králové
Katedra farmaceutické chemie a farmaceutické analýzy
Kandidát: Jorge Lozano Cañadilla
Školitel: prof. PharmDr. Petr Zimčík, Ph.D.
Název: Syntéza anionických ftalocyaninů

Tato diplomová práce je zaměřena na syntézu anionických ftalocyaninů s karboxylovými skupinami pro potenciální využití ve fotodynamické terapii (PDT). Studie nastiňuje význam rozpustnosti ve vodě při návrhu fotosenzitizérů pro účinnou PDT.

Syntetické postupy zahrnovaly různé reakce, včetně esterifikace, Suzuki-Miyaura cross couplingu a cyklotetramerizace, za účelem vytvoření ve vodě rozpustných sloučenin.

V experimentální části jsou podrobně popsány kroky, které byly podniknuty k získání konečných produktů, přičemž jsou zdůrazněny problémy, kterým bylo třeba čelit, jako jsou experimentální chyby a obtíže při separaci.

Sekce Výsledky a diskuse analyzuje výsledky a zdůrazňuje význam specifických reakčních podmínek a purifikačních technik.

Celkově tato práce přispívá k vývoji anionických ftalocyaninů s lepšími vlastnostmi pro PDT s cílem zvýšit jejich účinnost.

TABLE OF CONTENTS

ACKNOWLEDGMENTS

I would like to thank my supervisor Dr. Petr Zimčík Ph.D. for his time, for letting me use all the resources I needed and patience.

Also, I appreciate the help of Alex, Lucka and Eva. Their guidance and good atmosphere were key to complete the thesis.

Lastly, I want to thank all my new friends that I met here that were with me when I was doing my diploma thesis.

I declare that this thesis is my original author's work, which has been composed solely by myself. All the literature and other resources from which I drew information are cited in the list of used literature and are quoted in the paper. The work has not been used to get another or the same title.

Hradec Králové, 2024 Jorge Lozano Cañadilla

LIST OF ABREVIATIONS

AE: Adverse effect

ALA: Aminolaevulinic acid

CHF: Chloroform

DAMPs: Damage-associated molecular patterns

EAc: Ethyl Acetate

HPD: Hematoporphyrin derivative

Pcs: Phthalocyanine

PDT: Photodynamic therapy

PS: Photosensitizer

R_f: Retention factor

ROS: Reactive oxygen species

Rt: Room temperature

THF: Tetrahydrofuran

TLC: Thin layer chromatography

INTRODUCTION

Photodynamic therapy (PDT)

Photodynamic therapy (PDT) is based on a photochemical reaction between a light activatable molecule called photosensitizer (PS), light, usually in the visible spectrum, and molecular oxygen. When these three components are present together, reactive oxygen species are formed, which can directly damage cells and/or vasculature, and induce inflammatory and immune responses. This two-stage procedure significantly reduces side effects, as the harmless PS is activated only via directed illumination, resulting in local tissue destruction (1).

Photodynamic therapy (PDT) has shown promising results in cancer treatment, especially when combined with other therapies or immunostimulatory agents. However, there are still limitations and challenges to be addressed, such as standardizing treatment protocols, improving photosensitivity profiles of photosensitizers, and overcoming tumor hypoxia. (1)

Upon illumination, the PS absorbs a photon and is promoted to its excited singlet state, from which it can return to its ground state by converting its energy into heat or fluorescence. Alternatively, the PS can undergo intersystem crossing to its excited triplet state, where it can release its energy by phosphorescence or by colliding with other molecules to create chemically reactive species via two types of photoreactions: type I and type II reactions.

The figure 1 shows the two types of reactions. Type I reactions involve the PS reacting with an electron-donating substrate to form radical anion or cation species, which subsequently react with oxygen to form superoxide anion radical and other reactive oxygen species (ROS). In type II reactions, the excited triplet state of the PS reacts directly with ground triplet state oxygen to form highly reactive singlet oxygen.

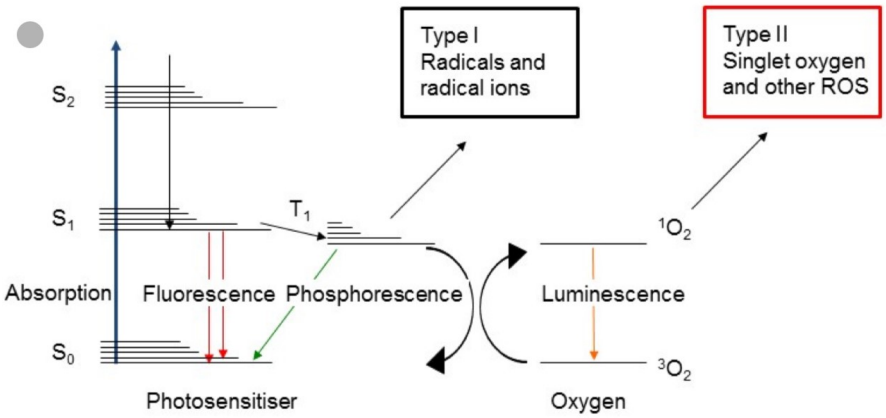

Figure 1: Schematic representation of type I and type II reactions. Reprinted from (1).

History

Oscar Raab and von Tappeiner first published accounts of what they termed a ‘photodynamic effect’ in 1900 and 1909, respectively. They described the ability of certain dyes to sensitize microorganisms to be killed by sunlight.

In 1948, Figge summarized a series of studies that indicated the retention of externally supplied porphyrins preferentially in murine tumors. This observation was extended to include human patients with cancer in 1955. The introduction of poorly defined hematoporphyrin resulted in visible fluorescence originating solely from the tumor. Clinical PDT advances took place in the Mayo Clinic. Its oncologists noted the differences in tumor and normal tissue fluorescence in patients when they employed a hematoporphyrin derivative (2).

A team, from the Medical College of South Carolina successfully replicated hematoporphyrin derivative. Expanding on this progress, Dougherty’s team at the Roswell Park Cancer Institute showcased hematoporphyrin derivatives ability to eradicate tumors in mice before transitioning to trials and reporting treatments. Referred to as PDT according to von Tappeiners terminology, this approach received FDA approval for treating cancer in 1995. Dougherty’s investigations uncovered HPDs tendency to accumulate in tissues and highlighted singlet oxygen as the primary agent responsible for cell destruction during PDT. Despite doubts, PDTs effectiveness in destroying tumor blood vessels led to its use in treating macular degeneration. However, the shift, towards commercializing PDT for this purpose diverted attention and resources from cancer research endeavors.

Prior, to 1991 literature on PDT mainly comprised studies. However, Pandey’s team at the Roswell Park Cancer Institute discovered that the active elements of hematoporphyrin derivative were porphyrin dimers and complex oligomers. This breakthrough eventually led to the creation of 'Photofrin' a derivative with applications, in settings.

It turned out that many such agents trigger cells to be light sensitized, so that when they selected their desired photosensitizer, they knew that there were certain sub-cellular parts which were affected by the molecule. Fluorescence microscopy allows observing this drug-delivery mechanism because the majority of the presently used agents are fluorogenic in nature.

Case Western Reserve University was the home of Oleinick’s group in 1991, finding apoptosis as a direct cell death pathway. Such a breakdown is often involved by this release of cytochrome c from damaged mitochondria or other sites in the cellular structure leading to targeting of Bcl-2, which is an important protein in this process.

The synthesis of a potent photosensitizer, termed benzoporphyrin derivative (BPD), at the University of British Columbia marked a significant advance, particularly in ophthalmic medicine. Another breakthrough came with Malik's finding that 5-aminolevulinic acid (ALA) could enhance protoporphyrin IX synthesis, with Kennedy’s group among the first to recognize its clinical potential.

The original photosensitizers, hematoporphyrin derivative and Photofrin, dissolve easily in water without needing special formulation. However, new ones are insoluble in water so requires liposomal delivery. This formulation can be modified to solely target lysosomes by binding new PS to a lipid before encapsulation. This allows for a single agent targeting of endoplasmic reticulum, mitochondria, and lysosomes, activated by a single light wavelength.

Targeting both mitochondria and lysosomes for photodamage enhances light-induced lethality. Additionally, targeting the endoplasmic reticulum (ER) can induce a new form of cell death (paraptosis) that affects cells with impaired apoptotic programs. (3)

PDT effect in cancer cells

At a cellular level, PDT can induce different forms of cell death, including apoptosis, necrosis, and autophagy, depending on the extent of cell damage and the localization of the PS.

Apoptosis is induced mainly when the PS goes to the mitochondria as it is a key organelle in this mechanism that when its membrane is permeabilized they liberate cytochrome When released into the cytoplasm from damaged mitochondria, it activates a number of proteins that lead to apoptosis, including caspases, which are enzymes responsible for triggering programmed cell death. Autophagy can occur when the lysosome is the main target. The necrosis is the most undesired one, as it is a process with worse regulation, that leads to the release of intracellular molecules that lead to inflammation. It can occur with higher doses, and when the PS alters the cell cycle.

PDT makes tumor destruction through direct effect on the cells by singlet oxygen and ROS, vasculature effects, and immune reactions. Although the therapy is not tumor cell-selective, the absence of lymphatics and enhanced permeation and retention effect (accumulation of macromolecules due to the increase in permeability in tumor's blood vessels) and PS characteristics contribute to its preferential accumulation in tumor tissue.

PDT impacts tumor cells and supporting tissue (stroma). While direct damage to cells is crucial, disrupting stroma, comprising 90% of tumor mass, is vital for effective treatment. However, PDT's efficacy is hindered by oxygen dependency, impacting poorly vascularized regions. Photosensitizer distribution, influenced by vascularity, varies, affecting responses.

Shortened intervals between PS administration and light activation enhance vascular damage. Intravascular PDT alters endothelial cells, inducing clotting factors, thrombus formation, and vessel occlusion, leading to tissue hypoxia and tumor destruction.

PDT also induces tumor destruction through inflammation and immune responses. Oxidative stress triggers heat shock proteins (HSPs) and inflammatory cytokines. Tumor cell death releases damage-associated molecular patterns (DAMPs), initiating

inflammation. PDT's ability to induce anti-tumor immunity has led to promising cancer vaccine research for prophylactic or therapeutic use. (1)

Factors affecting PDT effectiveness.

Light

PDT's effectiveness depends on light properties for PS activation. Light penetration into tissues varies due to their optical properties, limiting optimal wavelengths to 600-1300 nm. But light with wavelengths higher than 850 nm doesn't provide enough energy to activate the PS. So, in therapeutic the red region (620-850 nm) is the one used. (4)

Both lasers and incandescent light are the ones chosen, using specific ones based on PS characteristics, disease type, and practicality. Lasers, popular in clinical PDT, offer deep illumination, while LEDs show promise for cost-effective, broad-spectrum applications. Daylight use in PDT is under investigation, especially for superficial skin lesions. Light application methods, such as fluence rates and fractionation, impact outcomes and host anti-tumor reactions. (5)

Oxygen

Sufficient tissue oxygen is crucial for effective cancer therapy, and hypoxic areas in tumors are obstacles, impacting drug delivery and the efficacy of treatments like radiotherapy and certain chemotherapies. Hyperbaric oxygen therapy improves tumor response in chemotherapy and radiotherapy, but its impact on PDT varies among different photosensitizers. Thereby, it is important to know that oxygen depletion during PDT, influenced by light fluence rate, and vascular collapse further reduce tumor oxygenation, limiting the PDT efficiency. (1)

PS properties and localization (6)

The precise localization of PS is crucial for its therapeutic effect since the generation of ROS has a limited radius of action. The distribution of PS in tumor tissue, its association with serum proteins, extravasation from blood vessels and its association with the extracellular matrix or tumor cells are events that influence its final localization.

The charge, lipophilicity and structure of PS determine its cellular uptake and subcellular localization, which in turn affect its therapeutic efficacy.

The intracellular localization of PS is PS type-dependent and plays a significant role in cell fate, as different PS tend to localize to different cell organelles, which influences PDT-induced cell death mechanisms.

On the other hand, the charge distribution in PS may interfere with its availability and affect the electrostatic interaction with cell membranes, which influences its photodynamic efficacy.

PDT at specific tissues

Lung

PDT, especially with certain photosensitizers like sodium porfimer (Photofrin®) (figure 2), shows promise in endobronchial non-small cell lung cancer (NSCLC) and advanced NSCLC with central airway obstruction (7). Multimodal approaches, incorporating PDT with chemo-radiation therapy, demonstrate improved symptom relief, lung function, and survival rates.

PDT also proves beneficial in neoadjuvant and adjuvant therapies, increasing the eligibility for radical resection and improving mean survival time. Talaporfin-PDT, approved in Japan for lung cancer, combined with other therapies, significantly relieves airway obstruction, and enhances overall patient survival. Despite its effectiveness, Photofrin®-PDT has limitations, including prolonged skin photosensitivity and reduced efficacy for larger lesions. Second-generation photosensitizers like talaporfin and HPPH exhibit enhanced efficacy, making them promising alternatives (1).

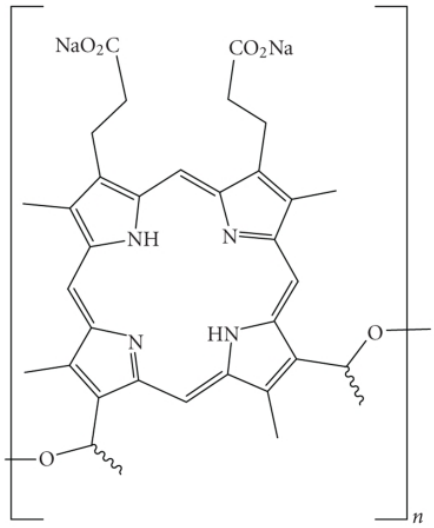

FIGURE 2: Photofrin. Reprinted from (7).

Esophagus

PDT, particularly with sodium porfimer (Photofrin®), shows curative potential for Barrett's esophagus (BE) and early esophageal cancer (7). It proves beneficial in adjuvant therapy for dysphagia, salvage treatment after failed therapies, and achieving long-term tumor-free survival in unfit surgery patients. However, post-PDT morbidities drive interest in alternatives like radiofrequency ablation and endoscopic mucosal resection. (8)

Skin

Skin cancers, divided into melanomas and nonmelanoma skin cancers, are mainly caused by UV radiation. Photodynamic Therapy (PDT) is a promising alternative, especially for nonmelanoma skin cancers. Early PDT research, starting in 1978, used haematoporphyrin derivative and evolved to second-generation PSs like aminolaevulinic acid (ALA), showing good outcomes with cosmetic benefits. Clinical studies compare ALA-PDT to surgical options, indicating comparable effectiveness with better cosmetic

outcomes. ALA-PDT is also explored for actinic keratosis, with outcomes comparable to other treatments but with some pain-related differences, making this a more painful option (1).

Female reproductive system

Reproductive cancers in women, such as uterine, cervical, ovarian, vaginal, and vulvar cancers, are commonly treated with surgery, chemotherapy, hormone therapy, or radiation. However, these standard therapies often carry side effects and increase the risk of pregnancy-related adverse events.

Succesful studies have been performed for peritoneal carcinomatosis and sarcomatosis, including ovarian cancer, and human papillomavirus. (1)

Head and neck

Head and neck cancers encompass diverse tumors affecting structures like the oral cavity, pharynx, larynx, and related areas. Traditional treatments include surgery, radiation therapy, and systemic therapies, each with limitations. PDT emerges as an alternative, particularly for early-stage and superficial tumors (9). Second-generation photosensitizers, such as 5-aminolevulinic acid demonstrate efficacy in treating precancerous and low-risk oral lesions, achieving complete responses with cosmetic benefits (10).

Bile duct

Bile duct cancer, a rare form of cancer, is difficult to diagnose early. Surgery is the best option but often not feasible due to late detection. Palliative treatments like photodynamic therapy (PDT) combined with biliary decompression can improve patient outcomes. Studies show PDT's effectiveness, especially with talaporfin, and its safety when combined with chemotherapy. Ongoing trials are exploring PDT's role in advanced cases. (1)

Bladder

The use of chlorin-e6 (Radachlorin®) in patients with high grade, nonmuscle invasive bladder cancer has proven effectiveness with low risk of adverse effects (11).

Pancreas

Pancreatic cancer, like bile duct and lung cancer, is often diagnosed at advanced stages. Tumor heterogeneity contributes to resistance against traditional therapies like radiotherapy and chemotherapy. Despite advancements in understanding its biology, pancreatic cancer remains challenging to manage, with less than 3% of patients eligible for curative surgery due to late diagnosis.

Photodynamic therapy (PDT) presents a promising alternative due to its ability to bypass many tumor resistance mechanisms.

One trial with Verteporfin® showed safe tumor reduction, suggesting PDT as a feasible and safe treatment option.

Photosensitizers

There are many different types of PSs. They can be classified into the first generation and the second generation depending on the selectivity of the molecule against cancer cells (figure 3), but the main group of molecules used in PDT are the ones with a tetrapyrrole structure. This group can be found in nature, for example, hemoglobin and chlorophyll. (12)

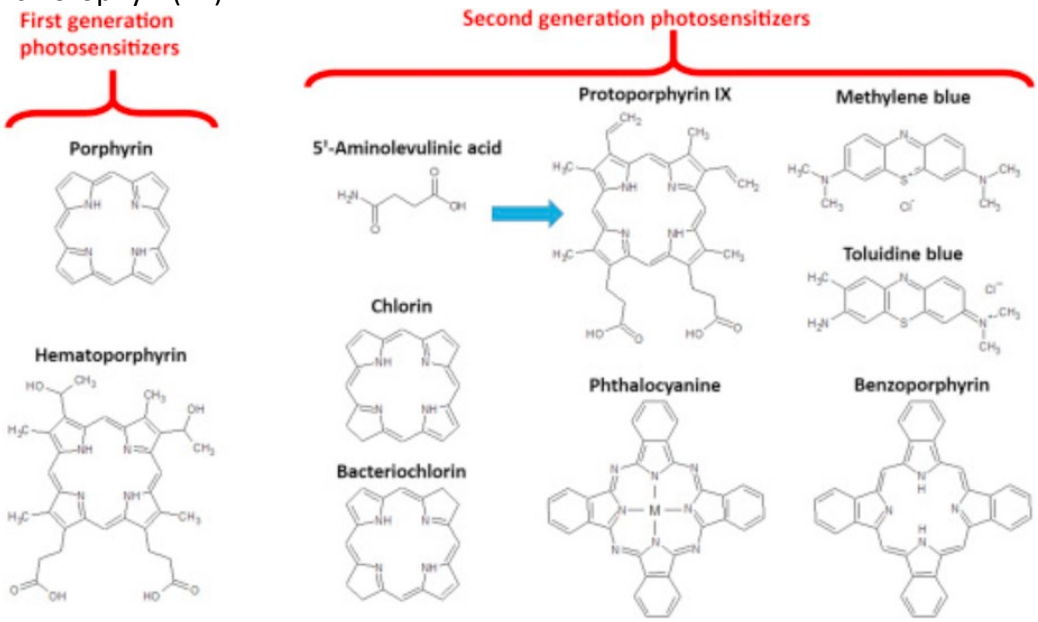

Figure 3: Structures of the main types of PS. Reprinted from (13).

Porphyrins

These PS were one of the first to be approved for PDT (14). Here we can find aminolevulinic acid (ALA), hematoporohyrin and its derivatives.

Although porphyrins are most effectively activated at the Soret band (~400 nm), their multiple Q-bands, extending up to the 630 nm region, make red light the common choice for in vivo porphyrin activation, though blue, green, or white light has been utilized for more superficial applications (15).

ALA is an amino acid that can be converted to protoporphyrin IX, a Pts, is extensively employed, particularly in dermatology (16). Esters of ALA have emerged as promising agents for PDT for several cutaneous tumors. In cancer cells, the ferrochelatase enzyme is not present, so prothoporphyrin IX is not degraded and consequently the ROS accumulate in the malignant cell. Both compounds are represented in figure 4

Figure 4: Representation of 5-ALA and Protoporphyrin IX. Reprinted from (17).

PDT with these derivatives has shown high response rates, excellent cosmetic outcomes, and low recurrence rates in patients with actinic keratosis, basal cell carcinoma, and squamous cell carcinoma. Furthermore, ongoing research aims to optimize PDT protocols and expand the use of ALA esters to other cancer types, highlighting their potential as valuable tools in cancer therapy. (18)

Hematoporphyrin derivatives, such as porfimer sodium (Photofrin®) have been defined by several features that are of immense clinical importance, being the foundation of photodynamic therapy. These techniques ensure that they tend to preferentially accumulate in malignant tissues, show specific wavelengths of light, and once exposed to light generate cytotoxic effects.

However, porfimer sodium (Photofrin®) is a varied mixture of molecules that shows, less tissue specificity, low absorption of light and, low penetration at the activation wavelength of porfimer sodium. A substantial quantity of porfimer sodium is required to attain the intended therapeutic objetive, resulting in extended circulation periods and prolonged patient photosensitivity.

After it's administration, hematoporphyrin derivatives accumulate markedly in cancerous tissues owing to their enhanced ability to uptake and retain while healthy tissues have lower uptake and retention levels.

Hematoporphyrin derivatives, like porfimer sodium, have already been clinically implemented in different types of photodynamic therapy (PDT) designs to manage cancer. Porfimer sodium has been the first choice in esophageal cancer treatment, and it also is the helpful drug for palliative treatment of obstructive endobronchial non-small cell lung cancer.

Chlorins

Chlorins are abundant in nature and vital for photosynthesis. Chlorins are particularly relevant for photodynamic therapy (PDT) due to their strong absorption in the 650-690 nm range, enabling deep tumor penetration with low toxicity and high stability and for their reduced circulation time making them more effective and safer. Clinically used chlorin-based photosensitizers include temoporfin (Foscan®), verteporfin (Visudyne®), chlorin e6 (Bremachlorin®, Photodithazine®), and talaporfin (Laserphyrin®). (19)

The chemical structure of chlorins can be modified to improve their properties for specific biomedical applications. For example, the introduction of different substituents or functional groups can alter their absorption spectra, enhance their solubility, or improve their targeting capabilities. Furthermore, the development of novel synthetic routes, such as the Diels-Alder reaction, has enabled the synthesis of diverse chlorin derivatives with optimized photodynamic activity and biocompatibility. (20)

Verteporfin, temoporfin and talaporfin, that are represented in figure 5, are one of the most important in this group.

Verteporfin is used in exsudative age-related macular degeneration, an illness that occurs because the eye is unable to eliminate the products of retinal metabolism and they accumulate between the retina and the choroid. This molecule reduces the new blod vessels. Talaporfin is indicated against lung cancer as Laserphyrin (21). Temoporfin is used in squamous cell carcinoma affecting the head or neck, when other treatments such as surgery, radiotherapy or chemotherapy cannot be used (22).

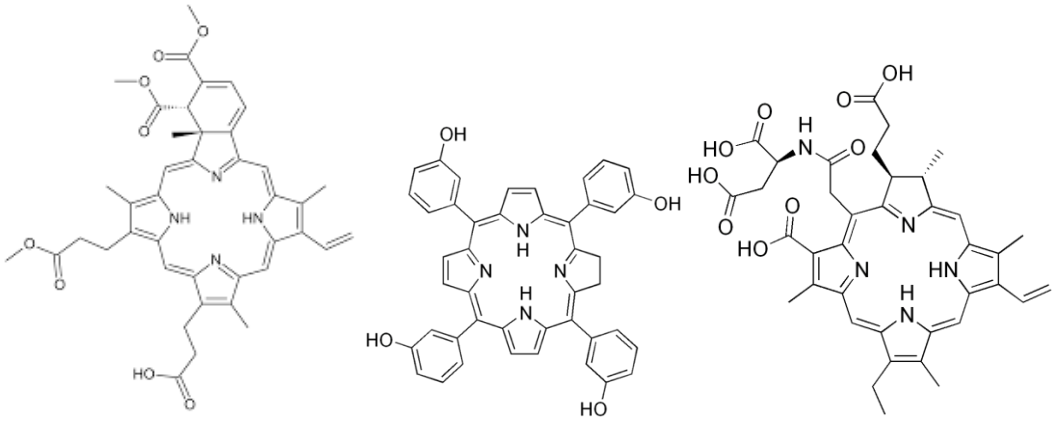

Figure 5: Structure of verteporfin, temoporfin and talaporfin.

Bacteriochlorin's

Some of them like padeliporfin (figure 6) is used for prostate and head and neck cancer (23). Infrared light between 700 and 800 is the optimal for this group (24). The main problem for these compounds is how easy it is to be degraded by light (25). However, there has been made new synthesis routes that minimize the inconveniences. One example is the union of dimethyl to each of the rings to avoid oxidation (25).

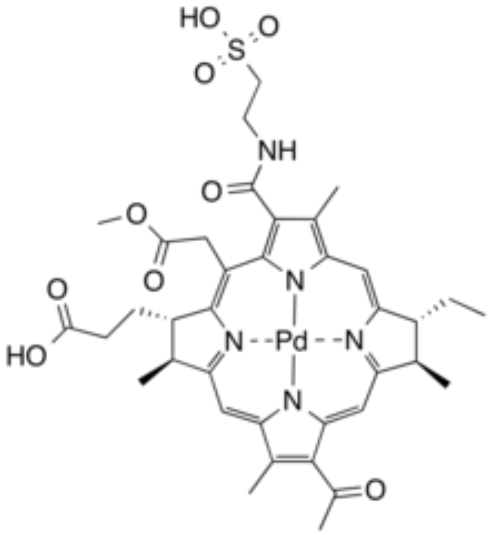

Figure 6: Example of bacteriochlorin - padeliporfin.

Phthalocyanines

This is the group of study in this project. They activate in a range of 650-720 nm. This makes it a great advantage as they absorb light optimal for penetration through the biological tissue. Their main inconvenience is that they are insoluble, so they tend to aggregate. Their properties will be discussed in detail in the following chapter.

Limitations of PDT

PDT has been proven effective for tumor treatments. However, despite its potential, there are limitations hindering PDT from becoming a standard care regimen for cancer treatment.

One major issue is the adverse events (AEs) associated with PDT, particularly with systemically administered photosensitizers. Skin photosensitivity, especially with first-generation photosensitizers, is a common AE, requiring patients to avoid sunlight and strong artificial light for extended periods. Pain is another frequently reported AE, with various factors influencing its occurrence, but effective pain management strategies remain elusive. Other AEs like inflammation, fever, and nausea are typically location-dependent but can be managed with medication.

Another drawback is the decreasing efficacy of PDT for larger lesions, especially with first-generation photosensitizers, due to inadequate tissue penetration of light or photosensitizer. Bulky or deep-seated tumors are challenging to treat with PDT, and even second-generation photosensitizers may perform less effectively in such cases.

PDT is not indicated for metastasizing tumors, as reaching metastatic sites with light is nearly impossible. Tumor recurrence is also a concern, possibly due to inadequate tumor eradication, insufficient penetration, or the presence of PDT-resistant tumor tissues, particularly in hypoxic environments.

Phthalocyanines

Phthalocyanine, an aromatic heterocycle composed of four nitrogen-bridged isoindoles, which is like porfirins, was first synthesized by Braun and Tcherniac in 1907. The central metal atom (usually transition metals like copper, nickel, or zinc) is coordinated to the nitrogen atoms, giving rise to a planar structure.

These highly conjugated systems impart strong near-infrared (NIR) absorption to phthalocyanine, primarily in the Q-band, centered between 670 and 850 nm, facilitating deep tissue penetration. Unlike clinically used porphyrins, which are prone to skin phototoxicity due to absorption peaks between 400 and 600 nm (B band), phthalocyanines exhibit minimal absorption in this range, reducing the risk of skin sensitivity.

Regarding their ability to produce singlet oxygen, Pcs are efficient photosensitizers due to their high singlet oxygen quantum yields. Singlet oxygen is generated through a process known as Type II photooxidation, where the excited state of the Pc transfers its energy to ground-state oxygen, forming singlet oxygen.

Substituents can be attached to the peripheral positions (on the benzene rings) or non-peripheral positions (on the isoindole units) of the Pc macrocycle, affecting their photophysical and chemical properties. Axial substituents can also be introduced, coordinating to the central metal atom, further modifying the properties of Pcs. These substituents can influence factors such as solubility, electronic properties, and reactivity, making them versatile platforms for tailored applications in fields like sensors, catalysis, and molecular electronics Pcs can be easily modified, allowing them to significantly change their photophysical and photochemical properties.

Currently, only one Pc (Photosens) is approved for clinical applications, while two others (Photocyanine and Pc 4) are in clinical trials. Photosens (figure 7), a mixture of sulfonated hydroxyaluminum Pcs, has shown promising results in treating cervical lesions. Photocyanine, a di(potassium sulfonate)-bis(phthalimidomethyl) zinc Pc, is under phase II trials in China, displaying high stability and therapeutic effects. Pc 4, a silicon Pc, has induced remission in animal models, but its insolubility requires suitable formulations for therapeutic efficacy.

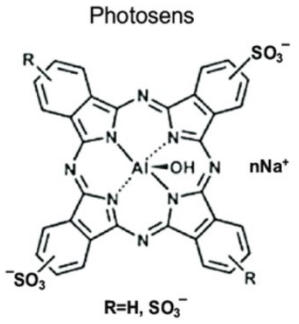

Figure 7: structure of sulfonated phthalocyanine Photosens.

Pcs, generally, have good characteristics such as low dark toxicity, high chemical and photochemical stability, minimal skin photosensitivity and high excitation wavelengths. But on the other hand, they are not soluble in most solvents. We can make Pcs more soluble in organic solvents by adding bulky substituents. On the other hand, the insolubility in water makes it incapable of producing the singlet oxygen because it tends to aggregate, making a change in the properties. Also, it makes impossible the entrance of the molecule to the cancer cell. That is the reason why the new research tends to add substituents that can be anionic or cationic (figure 8). (26)

Also, something important that determines the properties of the molecule is the metal that is in the center of the molecule. It has been shown that zinc is a metal that can allow the molecule to have the properties for the PDT. (27)

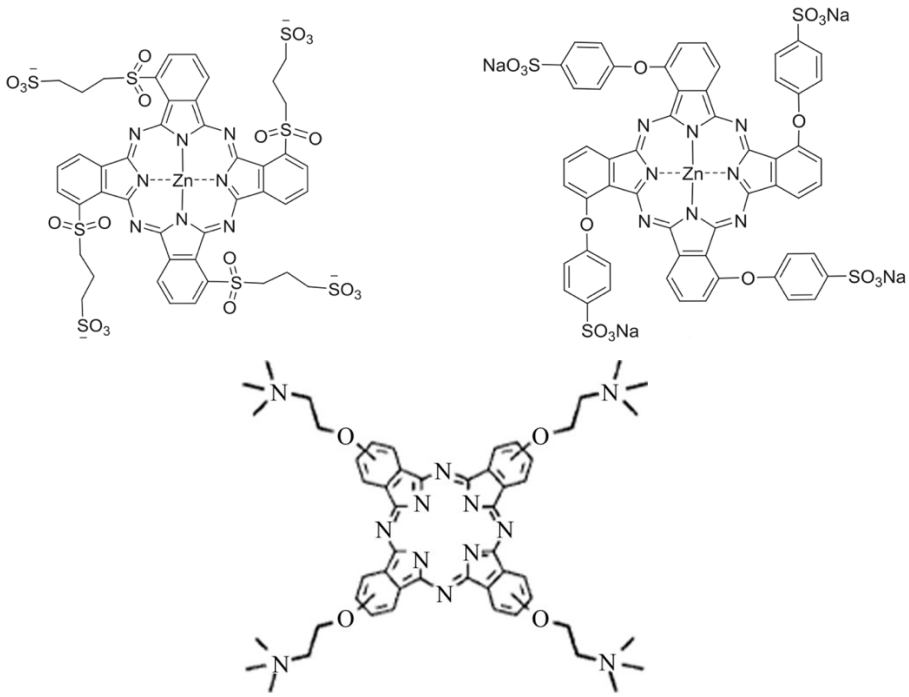

Figure 8: examples of tetrasubstituted anionic and cationic Pcs. Reprinted from (28).

Coupling reactions

These reactions are the most used for this research project.

A coupling reaction involves the joining of two atoms to generate a new chemical bond and give rise to a different molecule. These reactions are crucial in organic chemistry, as they enable the formation of C-C or C-heteroatom bonds.

These reactions require a transition metal catalyst to proceed at a practical rate in synthesis. Although several metals could, in theory, catalyze the different steps of these reactions, palladium (Pd)-based catalysts are the predominant ones.

Usually, it is chosen to start with palladium (II) species due to their superior stability. These compounds are reduced in situ to palladium (0) species, which participate in the catalytic cycle. The steps of the reaction mechanisms are widely recognized, and in particular, in the context of Pd complexes, are characterized by being organometallic in nature, occurring within the coordination sphere of the metal. (29)

AIM OF THE WORK

The aim of this thesis was the synthesis of anionic phthalocyanines, which contain carboxylic groups.

The Pcs are a group included in the second generation of PS that they have good photophysical properties for PDT: absorption around 700 nm (adequate for biological tissues) and high singlet oxygen production.

We chose these ones because having carboxylic groups it can be transformed to an anionic molecule so it can be more water soluble. This is important, because as mentioned above, phthalocyanines tend to aggregate in an aqueous medium when they are too lipophilic, changing their properties and nearly eliminating the possibility of forming the singlet oxygen. As the PS must be in water when it is administered, this is an important fact to control. The target compounds are represented in figure 9.

At the same time, these derivatives are suitable for further functionalization by reactions on the carboxylic functions. One of the running cooperations in the Azaphthalocyanine group is with Polish colleagues from Nicolaus Copernicus University Torun who are interested in attaching Pcs covalently onto biopolymers (e.g., chitosan). The target compounds therefore serve as starting materials for such functionalization.

Compounds of these final structures have already been prepared in Azaphthalocyanine group before and my task was to resynthesize them and check whether some improvements in the synthetic or purification method can be done. (30)

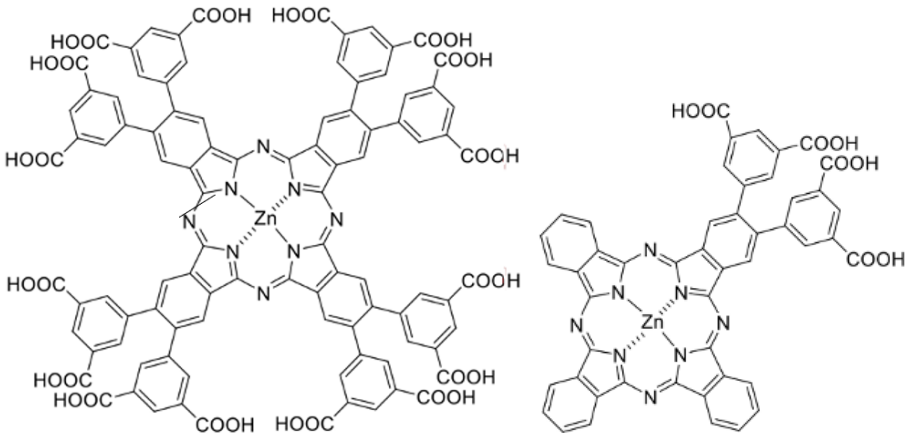

Figure 9: Representation of the compounds aimed to synthesize in this work.

EXPERIMENTAL SECTION

Material and instrumentation

Some of the starting materials were obtained from the lab from previous colleagues. Other chemicals and the solvents were purchased from Lach-Ner, Penta, Sigma-Aldrich, Merck or Acros. Butanol was stored over magnesium and distilled just prior to the use. For making thin layer chromatography (TLCs) we used Merck Kieselgel 60 F254 plates. The UV lamp was operating at 254 nm or 366 nm. For column chromatography, silica of Merck Kieselgel 60 (0.040-0.063 mm) was used. The NMR was done using Jeol JNM-ECZ600R or Varian S500. For size exclusion chromatography, a biobeads column (Bio-Beads S-X1 Support) with chloroform as mobile phase was performed.

Structures of the compounds synthesized.

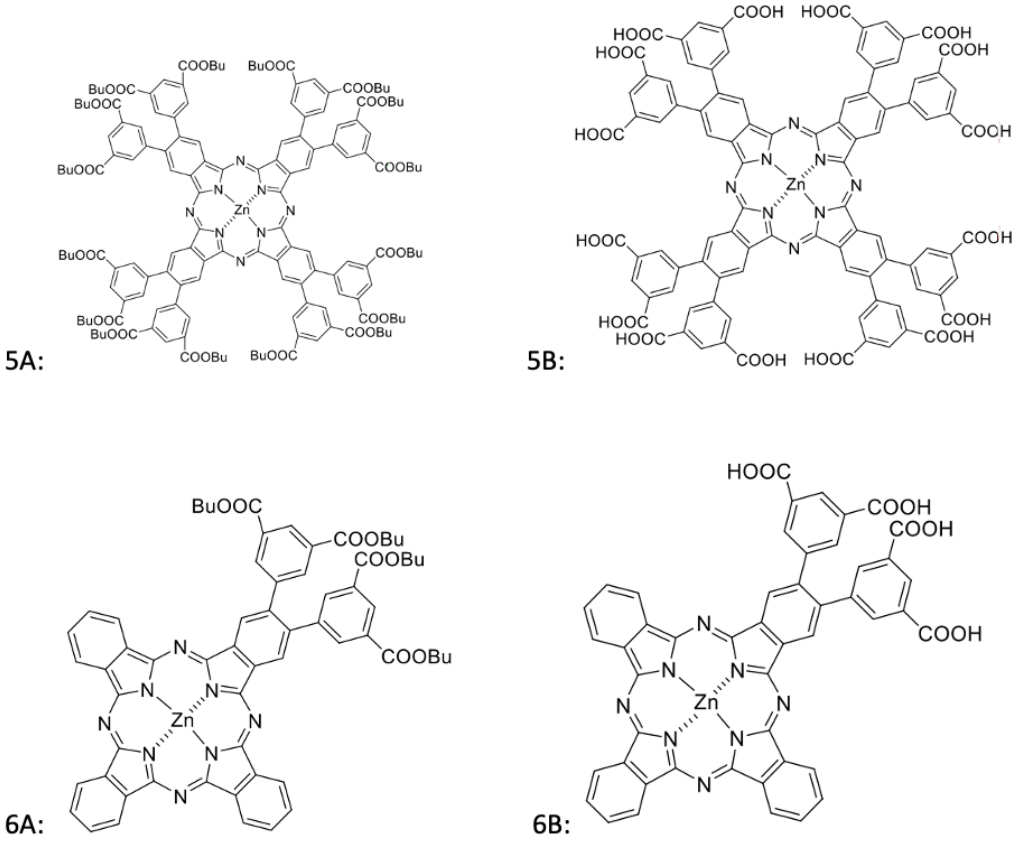

Figure 10. Structure of the main phthalocyanines with carboxylic groups for this thesis.

Reactions

Preparation of dimethyl 5-bromoisophthalate (2)

5-bromoisophtalic acid (**1**) (8.5 g, 0.034 mol), was added in methanol (50 ml), sulfuric acid (0.55 ml), and water (20 ml). The solution was stirred at 75 °C for 6 h. The mixture was monitored by TLC using hexane/ethyl acetate (5:1) as the mobile phase with the product`s standard (R_f= 0.6). Later, the reaction was cooled down, added dropwise to water (100 ml), and neutralized with NaOH (5%). The precipitate was collected and dried at 50 °C for one day. Yield 8.46 g (95 %). The reaction was performed according to the literature (31) and the product was confirmed by comparison with standard prepared before in the laboratory (31). The reaction is represented in figure 11.

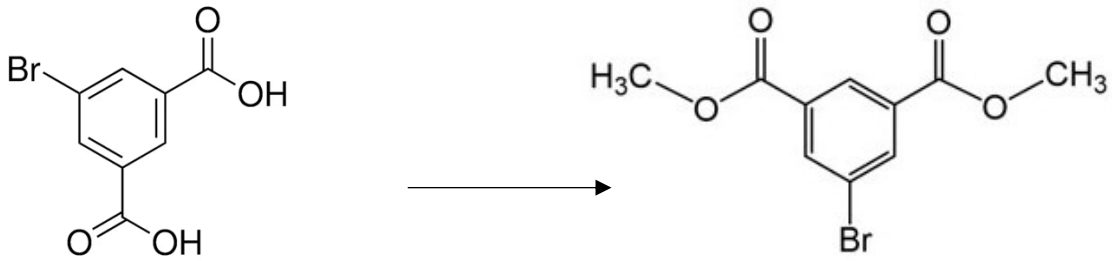

Figure 11. Synthesis of dimethyl 5-bromoisophthalate.

Preparation of dimethyl 5-(4,4,5,5-tetramethyl-1,3,2-dioxabor- olan-2-yl)isophthalate (3)

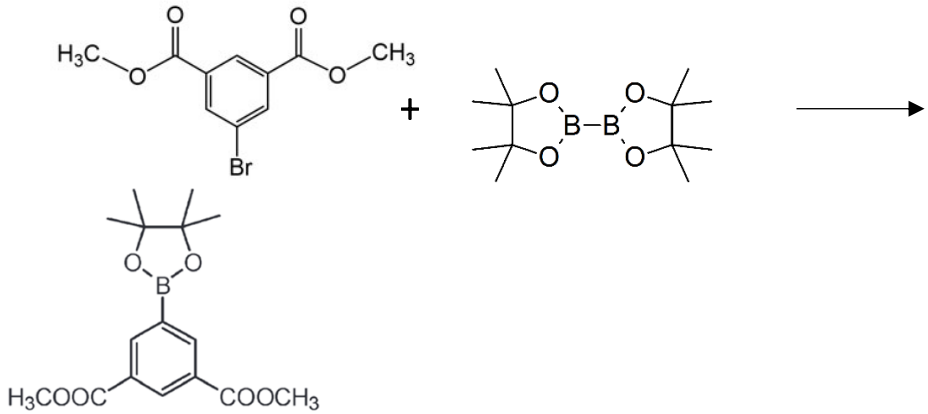

Figure 12. Synthesis of dimethyl 5-(4,4,5,5-tetramethyl-1,3,2-dioxabor-olan-2-yl)isophthalate.

Dimethyl dimethyl 5-bromoisophthalate (**2**) (2.7 g ,9.9 mmol), bis(pinacolato)diborane (3.0 g, 11.8 mmol), potassium acetate (2.8 g, 28.6 mmol), $PdCl_2(dppf)_2$ (0.1 g, 0.14 mmol), and dried 1,4-dioxane (20 mL) at 100°C were mixed for 20 hours. After that time, the reaction was poured into water (20 ml) and extracted by ethyl acetate. The

organic phase was collected and evaporated. The crude product was purified by column chromatography using hexane/ethyl acetate (3:1) as a mobile phase. The product (3) had a retention factor of 0.66 and a yield of 58% (1.85 g, 5.79 mmol) (32), (33). The product was verified aaccording to the literature (32).

The reaction is represented in figure 12.

Synthesis of 4,5-bis[3,5-bis(methoxycarbonyl)phenyl]phthalonitrile (4)

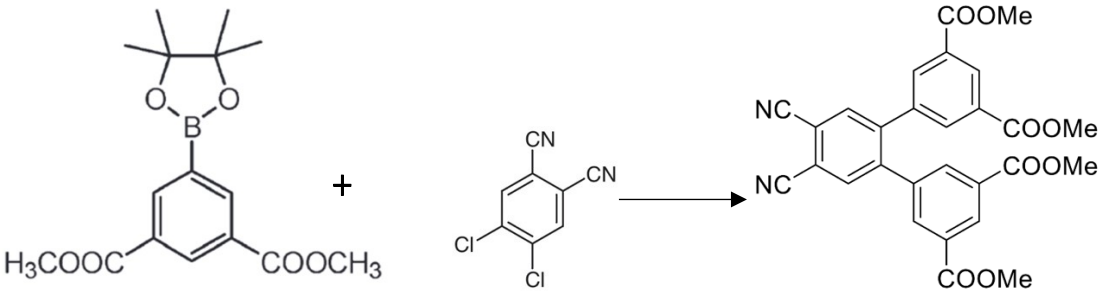

Figure 13. Synthesis of 4,5-bis[3,5-bis(methoxycarbonyl)phenyl] phthalonitrile.

Compound **3** (5.0046 g, 15.63 mmol), dichlorophtanonitrile (1.0549 g, 5.3 mmol), K_3PO_4 (3.253 g, 15.36 mmol), palladium (II) acetate (60.8 mg, 0.31 mmol) and XPhos (361.6 mg, 0.76 mmol) were introduced into a flask with THF (110 ml) under anhydrous conditions and stirred for 24h. Then, water (5 ml) was added and left for another 24h under argon. The organic solvent was evaporated, and the residue was extracted with ethyl acetate. The product was purified by column chromatography on silica with hexane/ethyl acetate (2:1) as the mobile phase and recrystallized from chloroform and methanol to obtain green crystals. Yield 68% (1.797 g, 3.50 mmol) (33)

The reaction is represented in figure 13.

^{1}HNMR (500 MHz, $CDCl_3$): δ 8.85 (s, 2H), 8.23 (d, J = 1.6 Hz, 4H), 8.24 (s, 2H), 4.03 (s, 12H).

Synthesis of 2,3,9,10,16,17,23,24-octakis[3,5-bis(butoxycarbonyl)phenyl]phthalocyaninato zinc(II) (5A)

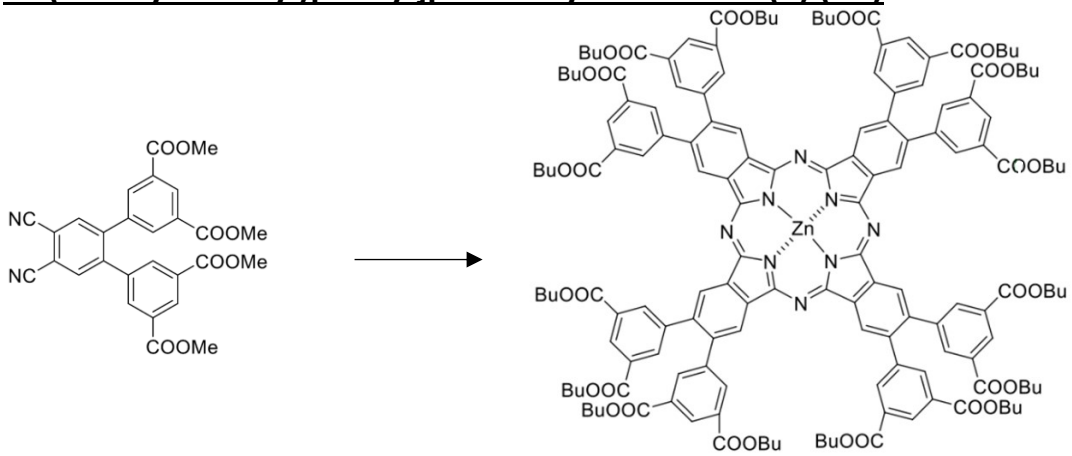

Figure 14. Synthesis of 2,3,9,10,16,17,23,24-octakis[3,5-bis(butoxycarbonyl)phenyl] phthalocyaninato zinc (II).

Magnesium (175.68 mg, 7.32 mmol) and small crystal of iodine were refluxed in anhydrous butanol (40 ml) for 5h until the magnesium butoxide was formed. Then, compound **4** (500 mg, 0.97 mmol) was added and left stirring for 20h. The mixture was cooled down and then reduced in the volume to half. Later, it was poured in water/methanol/acetic acid (25:25:1, 102 ml) and stirred for 1h to remove the unreacted magnesium. It was filtered to collect the green precipitate and washed with water.

A green precipitate (900 mg) was finally obtained. This precipitate was stirred with p-toluene sulfonic acid monohydrate (600 mg, 3,4 mmol) in THF (60 ml) for 1h at room temperature and evaporated. The solid was washed three times with water and three times with methanol.

A column chromatography was prepared with silica and toluene/THF (20:1) to collect the green product (R_f= 0.47). Then the product went through a second column, this time of bio beads to purify the product thanks to the difference in molecular weight.

The metal free ligand obtained (165 mg, 0,06mmol), and zinc acetate (30 mg, 0.156 mmol) were dissolved in pyridine (35 ml) and refluxed for 6h at rt. Then the solvent was evaporated and washed three times with water and three times with methanol. A column with chloroform/ethyl acetate (50:1) was made. To obtain the pure product it was recrystallized by adding dropwise the saturated solution of chloroform with 5A into methanol (10 ml). A blue solid was obtained with a yield of 21% (140 mg, 70 mmol)

The reaction is represented in figure 14.

^{1}H NMR (500 MHz, $CDCl_3$ /pyridine-d_5): δ 9.48 (s, 8H), 8.42 (t, J = 1.6 Hz, 8H), 8.31 (d, J =1.6 Hz, 16H), 4.05 (t, J = 6.6 Hz, 32H), 1.46 (m, 32H), 1.17 (m, 32H), 0.62 (t, J = 7.4 Hz, 48H).

^{13}C NMR (126 MHz, $CDCl_3$ /pyridine-d_5): δ 165.28, 154.15, 141.87, 140.40, 138.42, 131.09, 129.25,125.20, 65.00, 30.45, 18.99, 13.48.

Preparation of 2,3,9,10,16,17,23,24-octakis(3,5-dicarboxylatophenyl)phthalocyaninato zinc(II) (5B)

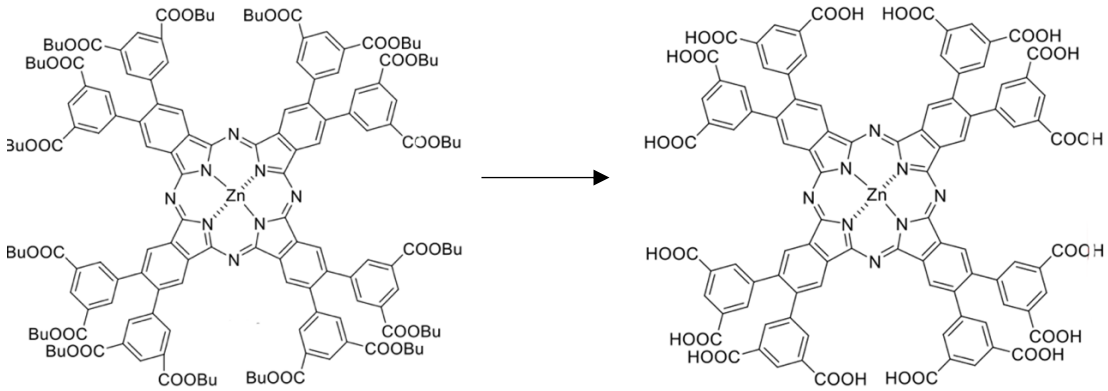

Figure 15. Synthesis of 2,3,9,10,16,17,23,24-octakis(3,5-dicarboxylatophenyl)phthalocyaninato zinc(II).

A saturated solution of NaOH in water/methanol (1:5, 60 ml) was prepared and **5B** (140 mg, 70.00 mmol) dissolved in THF (10 ml) was added dropwise, and left stirring for 4h at 40°C. After that, the green precipitate was filtered and washed with chloroform and methanol. The precipitate was dissolved in water and adjusted to pH=1 with HCl 1M. The formed precipitate was centrifuged at 8000 rpm for 10 minutes and carefully decanted and resuspended in water again. This procedure has been repeated 3 times. The solid was then dried and dissolved in the minimum of pyridine and dropped to diethylether. Then, it was filtered by vacuum to finish with a green solid with a yield of 63 % (70 mg, 37.27 mmol).

The reaction is represented in figure 15.

^{1}H NMR (500 MHz, DMSO-d_6): δ 13.24 (s, 16H), 9.53 (s, 8H), 8.39 (t, J = 1.6Hz, 8H), 8.22 (d, J = 1.6 Hz, 16H)

^{13}C NMR (126 MHz, DMSO-d_6): δ 166.66, 153.84, 147.91, 141.89, 140.45, 138.38, 135.50, 131.65, 125.09

Synthesis of 2,3-bis[3,5-bis(butoxycarbonyl)phenyl]phthalocyaninato zinc(II) (6A)

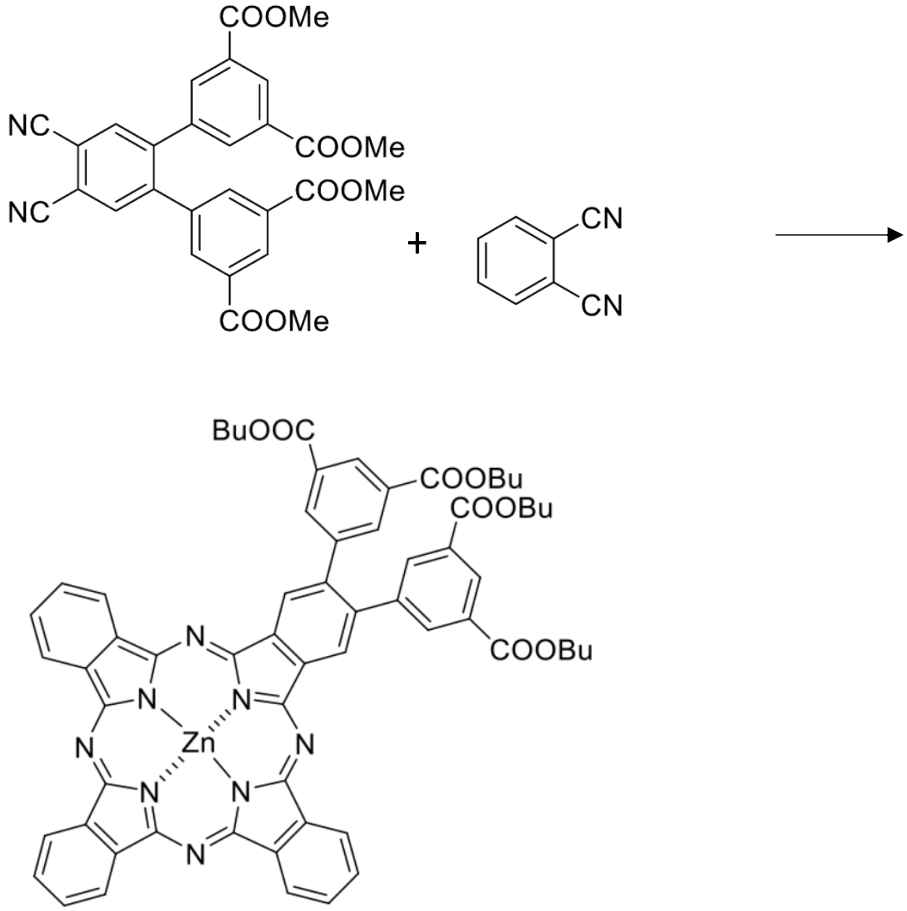

Figure 16. Synthesis of 2,3-bis[3,5-bis(butoxycarbonyl)phenyl]phthalocyaninato zinc(II).

Mg (328.36 mg, 13.60 mmol) and small crystals of iodine were refluxed in butanol (17 ml) for 5h to create magnesium butoxide. At this moment, compound **4** (250 mg, 0.49 mmol) and phthalonitrile (187.5 mg, 1.09 mmol) were added and then it was kept refluxing for 20h. The mixture was removed from the reflux and cooled down. When it reached the room temperature, it was partially evaporated and then poured into a mixture of water/methanol/acetic acid (25:25:1, 102 ml). The precipitate was collected and washed with water and methanol. TLC of CHF/THF (50:1) showed products with these R_f: 0.82, 0.73, 0.63, 0.09 and 0. With a column chromatography with chloroform as mobile phase some of the impurities were removed, but the mixture showed several spots in all the TLC with Rf: 0.45, 0.55 and 0.58.

This crude product (302.3 mg) was added to p-toluene sulfonic acid hydrate (600 mg, 3.17 mmol) dissolved in THF (30 ml) to form the metal-free ligand. The solution was stirred for 2 h, and the evaporated by reduced pressure to remove the THF.
The metal-free ligand (228.8 mg, 214.03 mmol) and zinc acetate (280.46 mg, 1.46 mmol) were dissolved in pyridine (26 ml) and then refluxed 6 h to create the zinc complex. First, a column with chloroform was made. Later, a column with bio beads. Then, another one with chloroform/methanol (400:1). Finally, it was purified with a column of

CHF/THF/EAc (60:1:1) to give a green solid. R_f: 0.54. The final yield was 21 % (89 mg, 78.13 µmol).

The reaction is represented in figure 16.

^{1}H NMR (500 MHz, $CDCl_3$/ pyridine-d_5): δ 9.32 (m, 4H), 9.22 (m, 4H), 8.91 (s, 2H), 8.68 (d, J = 1.6 Hz, 4H), 8.12 (dd, J = 5.6, 2.8 Hz, 2H), 8.08 (m, 4H), 4.43 (t, J = 6.6 Hz, 8H), 1.86 (q, J = 8.0, 7.4 Hz, 8H), 1.56 (m, 8H), 1.07 (t, J = 7.4 Hz, 12H).

^{13}C NMR (126 MHz, CDCl3/ pyridine-d5): δ 165.45, 153.72, 153.47, 152.70, 151.35, 142.24, 138.96, 138.37, 138.31, 138.11, 137.63, 135.55, 131.06, 129.12, 129.05, 128.92, 124.56, 65.06, 30.55, 29.49, 29.25, 23.81, 19.09, 13.56.

Preparation of 2,3-bis(3,5dicarboxylatophenyl)phthalocyaninato zinc(II) (6B)

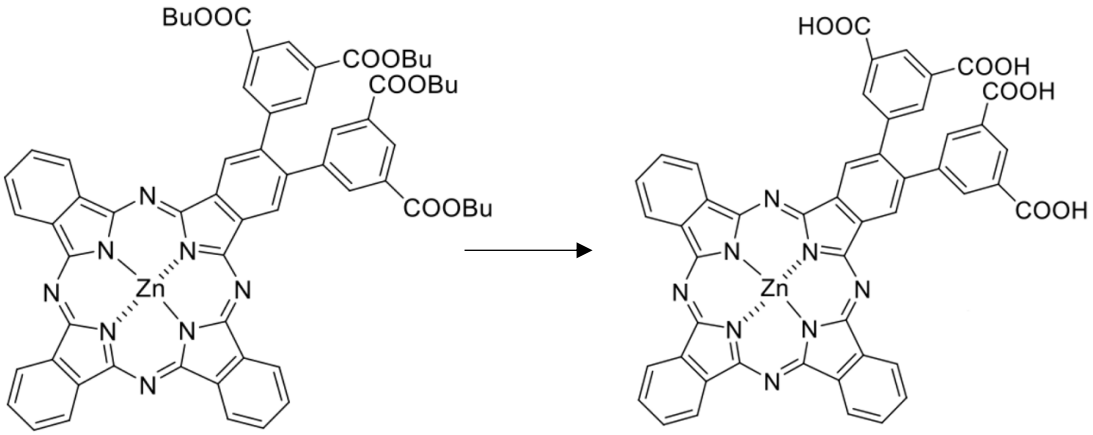

Figure 17. Synthesis of 2,3-bis(3,5dicarboxylatophenyl)phthalocyaninato zinc(II).

Compound **6A** (89 mg, 78 µmol) was dissolved in THF (7 ml). Then it was added to a saturated solution of NaOH in water/methanol (1:5, 40 ml) that was previously prepared. The mixture was left stirring for 4h at 40°C. When the precipitate was formed and collected, it was dissolved in water and acidified with a solution of HCl 1 M until pH 1. The precipitate was first filtrated, then suspended in a 0.001M HCl solution, centrifugated, decanted for 3 times. The blue solid was obtained. Yield 73% (51.80 mg, 1.4 µmol).

The reaction is represented in figure 17.

The results were verified by NMR:
1H NMR (500 MHz, $CDCl_3$/ pyridine-d_5): δ 1.95 (s, 13.34 H), 3.90 (d, J = 9.40, 9.36 Hz), 4.02 (s, 8.57 H), 3.98 (d, J = 8.51 Hz), 2.01 (t, J = 8.36, 8.35, 8.33 Hz), 1.01 (s, 7.95 H), 1.00 (s, 7.78 H), 2.01 (t, J = 7.39, 7.38, 7.37 Hz).

DISCUSSION OF THE RESULTS

As mentioned before, the aim of the thesis was to synthesize anionic phthalocyanines, which are the ones that have carboxylic groups. These types of Pcs are more water soluble, so they don't aggregate, losing their capacity to produce singlet oxygen. At the same time, carboxylic functions allow simple modification by formation of esters or amides.

The compounds to synthesize could be divided in anionic hydrophilic and anionic amphiphilic. The structural difference between them is the number of carboxylic acids that the molecule has. This makes them have differences in some of their properties.

The scheme of all the reactions to make was:

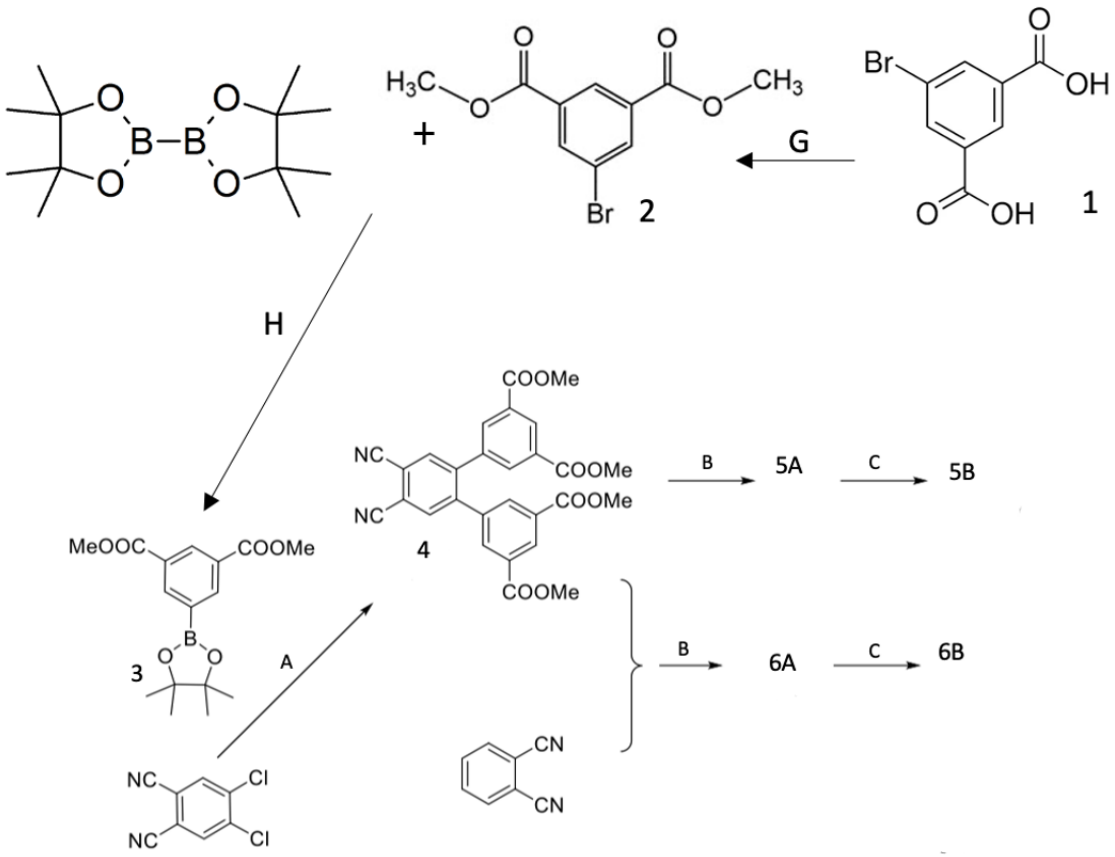

Scheme 1. Reaction conditions: **A**: K_3PO_4, $Pd(AcO)_2$, XPhos, THF/water. **B**: Mg, BuOH, reflux; then p-TsOH, THF rt; then $Zn(AcO)_2$, pyridine, reflux. **C**: NaOH, water/MeOH/THF, rt; then HCl. **G**: MeOH, H_2O, H_2SO_4, heat; H_2O, NaOH 5%. **H:** bis(pinacolato)diborane, potassium acetate, Pd, dried 1,4-dioxane.

5A:

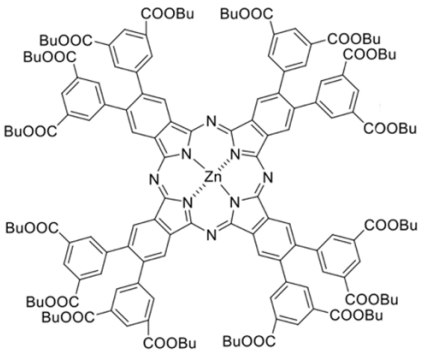

5B:

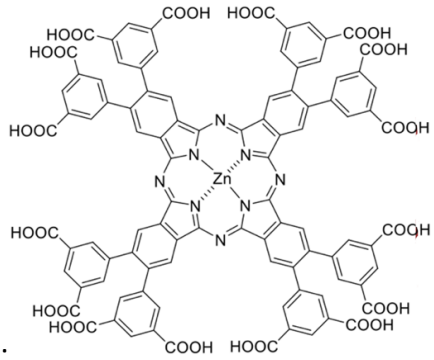

6A:

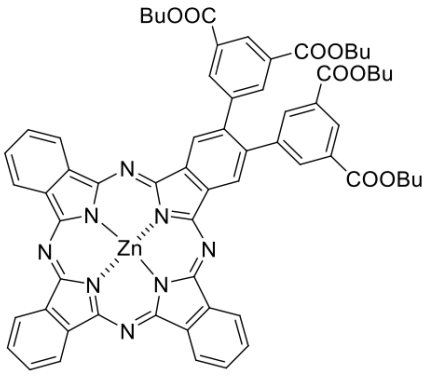

6B:

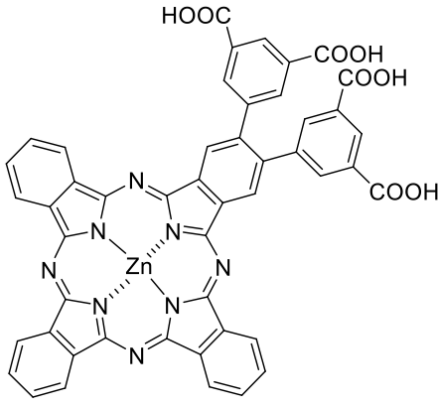

The synthesis of these compounds was performed before in the literature (31) and was made to have it as a precursor for the following reactions.

We started with a small amount of 5-bromoisophtalic acid to ensure the successful execution of the reaction as outlined in the literature. 5-bromoisophthalic acid was dissolved in methanol and sulfuric acid, utilizing the protonated alcoholic group necessary for esterification (Figure 18). Additionally, heat was applied as typically required.

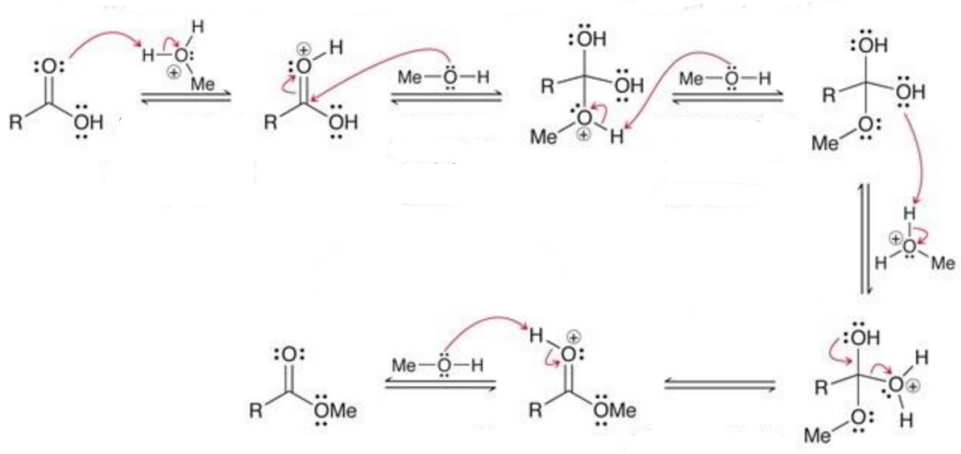

Figure 18. mechanism of a Fischer esterification.

During this reaction, we employed a reference compound available in our laboratory for thin-layer chromatography (TLC) using a hexane/ethyl acetate (5:1) solvent system. This facilitated comparison between our TLC results and those reported in the literature, providing standards for both the reactant and the product.

Finishing the reaction, the mixture was introduced in water to induce precipitation of the product, due to the low water solubility of esters.

Initially, the reaction yielded only 50%. However, subsequent repetition of the reaction with increased reactant quantities resulted in a 95% yield, slightly higher that reported in the literature (32).

In the next step, we followed by preparation of boronic acid pinacol ester **3.**

Compound **2** was subjected to reaction with bis(pinacolato)diborane, with a Suzuki reaction (figure 19) employing potassium acetate as a base and $PdCl_2(dppf)_2$ as a common catalyst for this, using dried 1,4-dioxane as the solvent.

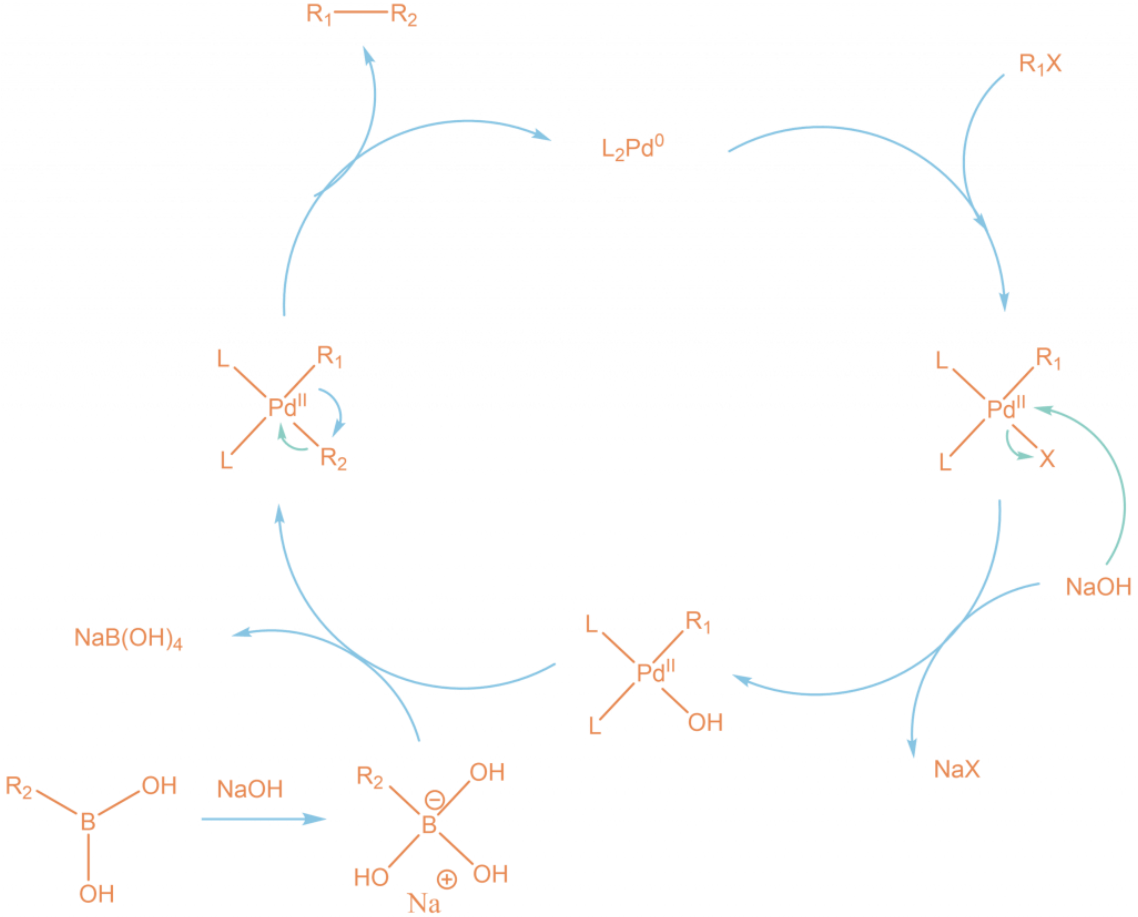

Figure 19. Mechanism of Suzuki reaction. Reprinted from (34).

As the product has low polarity, it was subjected to extraction with ethyl acetate to isolate organic phase, which was then dried. However, undesired organic compounds persisted. To address this, a column chromatography of hexane/ethyl acetate (3:1) was

used for purification. The yield was 59 %, slightly lower than the previously reported (32). As it was done before by one of my colleagues and it was already done in the literature, no NMR was deemed unnecessary.

Compound **3**, being a favorable substrate for coupling reactions, was subjected to a Suzuki-Miyaura reaction with dichlorophthalonitrile, K_3PO_4, and palladium acetate in THF. The reaction was conducted under anhydrous conditions, with argon atmosphere to eliminate oxygen. This process entails the formation of a carbon-carbon bond between the aryl group of **3** and 4,5-dichlorophthalonitrile, catalyzed by palladium. The Suzuki-Miyaura cross-coupling reaction represents a widely employed method in organic synthesis for the construction of carbon-carbon bonds (figure 20).

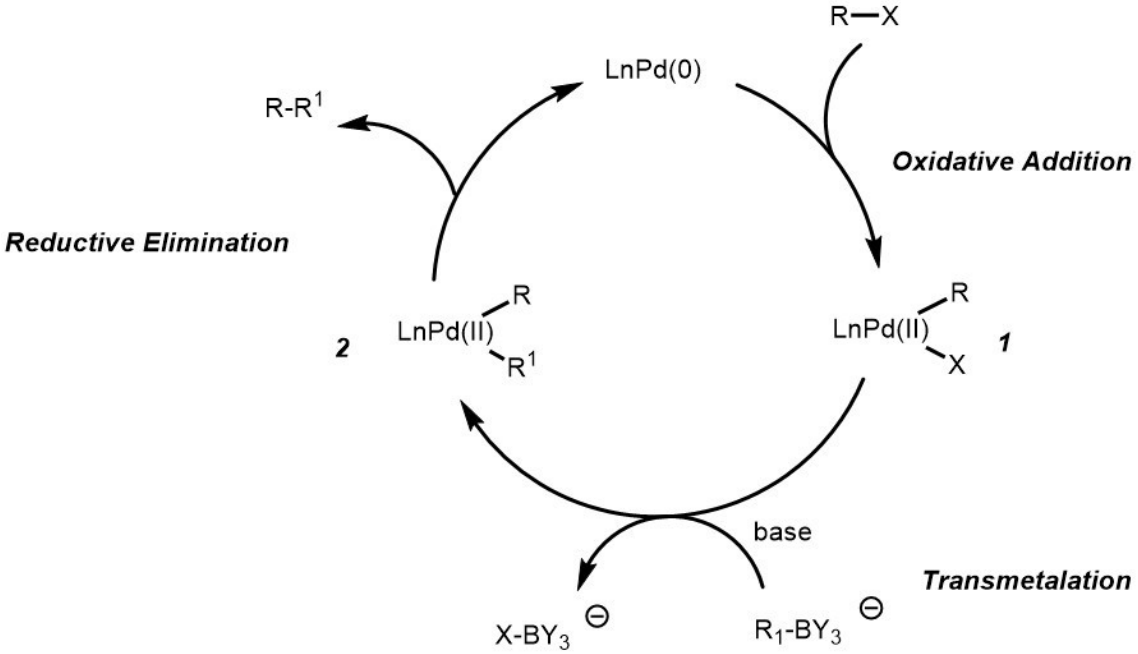

Figure 20. Mechanism of Suzuki-Miyaura reaction. Reprinted from (34).

Subsequently, the product was purified by column chromatography using hexane/ethyl acetate (2:1) followed with a recrystallization with chloroform and methanol. This procedure was repeated twice to obtain additional starting material for subsequent reactions. The first yield obtained was 59%, while the second was 68%, both of which were lower than those reported in the literature (30), possibly attributable to experimental errors.

With the phthalonitrile precursors at hand, the subsequent step involved the synthesis of phthalocyanines through cyclotetramerization—a process characterized by intramolecular cyclization, initiated by magnesium butoxide.

The reaction started by stirring the magnesium, iodine, and butanol to form magnesium butoxide, with iodine serving as a magnesium activator. Subsequently, compound **4** was introduced into the reaction mixture, and the system was left stirring for 20 hours.

Then the mixture was cooled down and concentrated, preparing it for immersion in a solution of water/methanol/acetic acid (25:25:1) and stirred for 1h to remove the excess of magnesium butoxide. Subsequently, the magnesium complex underwent demetallation using p-toluenesulfonic acid monohydrate in THF as the solvent for 1 hour. This acid-mediated process facilitated the removal of magnesium from the molecule, as the desired properties for PDT necessitated the formation of the zinc complex.

The process of initially forming the magnesium complex followed by conversion to the zinc complex in the synthesis of the **5A** compound was chosen for its enhanced efficiency in organic synthesis. Previous studies have demonstrated the effectiveness of this strategy in synthesizing phthalocyanines and their metal complexes. Importantly, the cyclotetramerization in butanol led to the transesterification and introduction of butoxy groups into the phthalocyanine structure, which is crucial for physico-chemical properties. Larger butyl esters exhibited less aggregation compared to methyl esters, thereby enhancing product solubility.

Following the formation of the metal-free molecule, column chromatography was employed to separate various compounds. The first one was a column chromatography with toluene/THF (20:1) as a mobile phase. However, the product obtained was impure, necessitating a subsequent purification step using exclusion chromatography with biobeads in a second column chromatography to achieve final purity. Biobeads were preferred due to their separation based on molecular weight rather than polarity.

Subsequently, the product obtained, and zinc acetate was then refluxed for 6h in pyridine. Zinc acetate served as the source of zinc while, pyridine an organic solvent adequate for organic reactions that also can acted as a base. The resulting solid was then washed with water and methanol to remove some impurities. A column chromatography with chloroform/ethyl acetate (50:1) as mobile phase yielded a product that was nearly pure upon TLC analysis. For that reason, recrystallization with methanol was needed to purify it.

The yield of the final product was 21%, which was lower than the yield reported in previous experiments. This decrease in yield could be attributed to an accident involving a flask containing the compound.

Additionally, during the first chromatography procedure, a solid formed unexpectedly, causing the column to become clogged. Consequently, we had to repeat the process, washing the silica with chloroform to remove the compound, which proved challenging due to the tendency of phthalocyanines to adhere to silica.

The chemical mechanism for the conversion of compound **5A** to compound **5B** involves the hydrolysis of the butoxy groups present in compound **5A** to form carboxyl groups. This process is carried out by reaction with a sodium hydroxide solution in a mixed solvent system of water and methanol.

Initially, compound **5A** was dissolved in tetrahydrofuran (THF) and slowly added to a saturated solution of sodium hydroxide in water/methanol (1:5). The presence of the strong base, in this case sodium hydroxide, promotes the cleavage of the butoxy ester bonds present in the compound **5A**. This hydrolysis process leads to the formation of the carboxyl groups instead of the butoxy groups. The reaction was carried out at a temperature of 40 °C for 4 hours to ensure complete conversion of compound **5A** to compound **5B**. The crude product was subsequently converted to its free acid form through acidification with hydrochloric acid until reaching a pH of 1 that made the compound insoluble in water. Despite the addition of a substantial amount of HCl, the solution did not exhibit immediate precipitation. However, upon centrifugation, a very fine precipitate became evident at the bottom. The precipitate was then centrifuged, decanted, and resuspended with HCl 5% 3 times. The precipitate formed was collected by filtration, yielding compound **5B.** The yield was 63 %, lower that the one reported in the article (30).

The next compound to synthesize was **6A.** In this reaction, two starting phthalonitrile derivatives enter the reaction leading to mixture of six compounds which are represented in figure 21. And each one had a specific color, because they had different substituents that influenced absorption spectrum and consequently also the color.

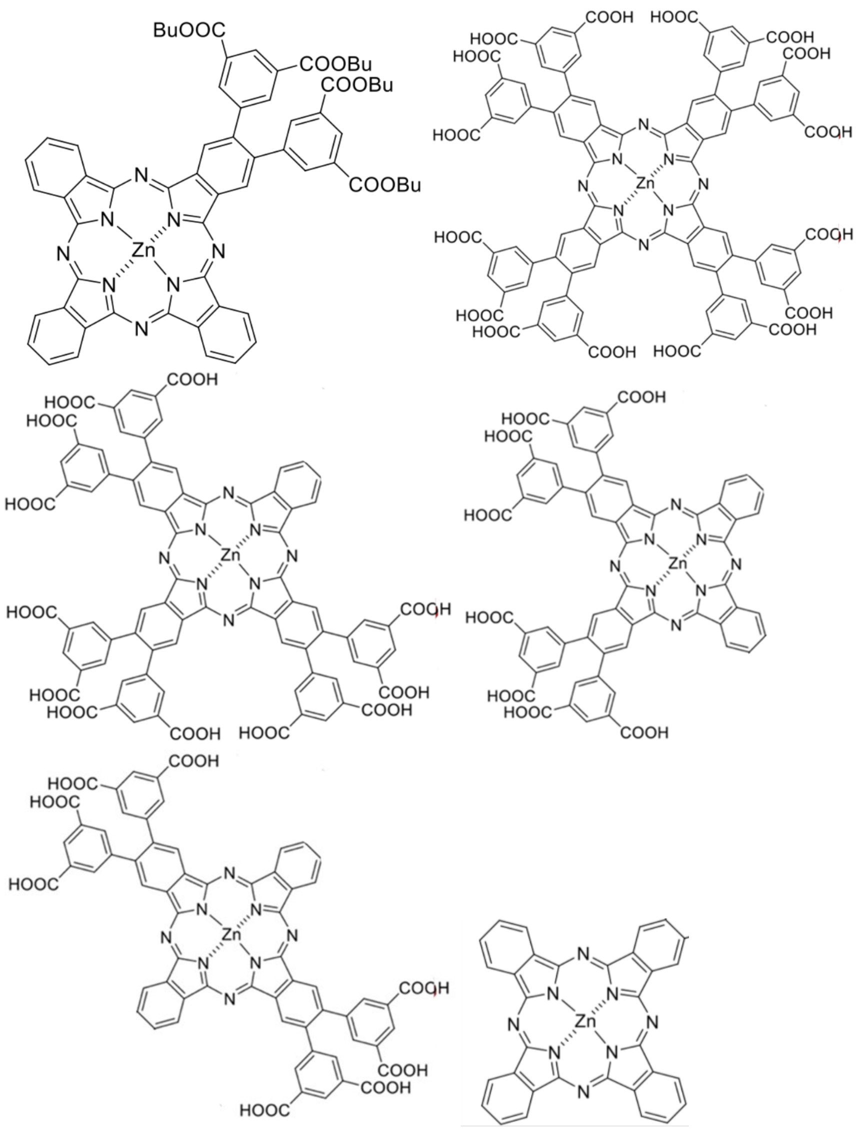

Figure 21. Representation of the six main products in the synthesis of **6A.**

The mechanism of the formation of this compound is similar as for the compound **5A**. The main difference is that compound **6A** is formed as an asymmetric compound due to the use of a statistical condensation approach in the synthesis. This means that the reactives tend to distribute randomly, leading to the formation of a product containing a mixture of different functional groups.

That is why more than one product is formed when magnesium, **4** and phthalonitrile are combined. The three compounds need to be separated carefully.

Before proceeding with the column chromatography, it was necessary to wash it with a mixture of water and methanol to remove any unreacted magnesium butoxide.

This reaction had to be prepared three times to be completed.

In the first time, we started with of **4** and 3 times the amount of moles of phthalonitrile. This was subjected to a condensation reaction in the presence of magnesium butoxide as initiator. During this step, the magnesium complexes occurred. However, upon attempting chromatography, difficulties arose in determining the appropriate mobile phase due to the challenges associated with separating phthalocyanines. The first one was with chloroform/THF (20:1), without any visible results in the separation. Subsequently, another attempt was made using CHF/THF (30:1) as the mobile phase, but this endeavor also proved unsuccessful. After several unsuccessful trials with different mobile phases and TLC analyses, it was determined that a mixture of CHF/Toluene/THF (20:20:1) provided significant separation. Therefore, employing this mobile phase in the chromatography enabled successful separation of the fractions.

In the subsequent step, the magnesium complex formed in the previous reaction was converted to the metal-free derivative through stirring with p-toluenesulfonic acid in THF at rt. Purification of the product did not necessitate chromatography, as the only contaminant present was the acid. Instead, purification was achieved through extraction with ethyl ether and water. During this stage, one incident with the flask occurred, loosing part of the compound.

Then the metal-free ligand is converted into the zinc complex by the addition of zinc (II) acetate in pyridine refluxing for 6h. This conversion is performed to introduce the zinc atom into the structure of the compound, resulting in the formation of the **6A** zinc complex. However, the yield obtained after this step was insufficient, necessitating the repetition of the procedure.

For the second attempt, we followed another strategy which consisted of making the zinc complex the same way but doing it directly without intermediate column separations. When the zinc complex was formed, we explored several different separation methods. Initially, it was with CHF/Toluene/THF (20:10:1) but we couldn't proceed. The second time, was with a column only with chloroform, followed by another one with bio beads. Finally, a preparative TLC was made with CHF/THF/Ethyl Acetate (30:1:1) as mobile phase. The silica with the product was scratched, filtrated, and evaporated. Although the separation was successful, the yield was insufficient, requiring one more repetition of the process.

For the last time, we started with the same amount and proceeded the same way again, but now a chromatography was made with the metal free form of the compound. Although some compounds were successfully separated using chloroform, the presence of additional compounds rendered the purification insufficient.

Nevertheless, we proceeded with the reaction of the zinc complex, because we though that the compound could be separated in the next step.

First, we attempted with a column with CHF. However, we observed that the mobile phase was too nonpolar, necessitating an increase in polarity. Subsequently, we

employed another column with CHF/methanol (400:1) as the mobile phase, resulting in improved and faster separation due to the enhanced polarity with methanol.

Finally, for purification, we conducted another chromatography using CHF/THF/Ethyl acetate (60:1:1) based on our TLC observations, which indicated effective compound separation.

Following the reaction, we proceeded hydrolysis of the ester bonds. This reaction closely resembled the procedure for compound **5B**, as the objective remained consistent: to remove the esters, leaving behind an acid group that could be converted into a water-soluble salt. This transformation is crucial for preventing the aggregation of phthalocyanines when administered to patients, as they must be dissolved in an aqueous medium.

To finish with the procedure, **6A** was dissolved in THF to be transferred to 40 ml of a saturated solution of NaOH in water/methanol (1:5) and it was stirred for 4h in a beaker. Then, it was precipitated from the solution by acidifying with HCl 1M until pH 1. The resulting precipitate was then filtered, suspended in a 0.001M HCl solution, centrifuged, and decanted three times for purification.

CONCLUSION

The aim of this work was the synthesis of anionic of photosensitizers with carboxylic acids, in particular, phthalocyanines, so they can be transformed and be more water soluble or modified by targeting moieties.

The work started by preparing the precursors. The first reaction was the synthesis of ester of 5-bromoisophthalic acid. It was done two times, because the first try was to check that the procedure was correct, and the second time to proceed with the reaction giving successful results. Then, the Suzuki reaction was started to make the boronylated derivative suitable for coupling reactions. The reaction gave yield slightly smaller than the one described in the literature.

The synthesis of substituted phthalonitrile was performed via Suzuki-Miyaura cross-coupling reaction, a typical reaction for forming C-C bonds. Giving good results when looking to the NMR, but with small yields compared to the ones done it before.

When all the precursors were done, the phthalocyanines synthesis of symmetrical phthalocyanine was simpler and the results from the NMR and yields were as expected. But for the unsymmetrical derivative, because of the difficulty of separating them, the procedure had to be repeated for three times till the NMR and yield had the value expected.

REFERENCES

1. Van Straten, D.; Mashayekhi, V.; de Bruijn, H. S.; Oliveira, S.; Robinson, D. J. Oncologic Photodynamic Therapy: Basic Principles, Current Clinical Status and Future Directions *Cancers* **2017**, *9*, 19. https://doi.org/10.3390/cancers9020019

2. Detty, M. R., Gibson, S. L., & Wagner, S. J. Current clinical and preclinical photosensitizers for use in photodynamic therapy. *Journal of Medicinal Chemistry*, **2004**, *47*: 3897-3915. https://doi.org/10.1021/jm040074b

3. Kessel, D. Photodynamic Therapy: A Brief History *J. Clin. Med*. **2019**, *8*, 1581. https://doi.org/10.3390/jcm8101581

4. Szacilowski, K.; Macyk, W.; Drzewiecka-Matuszek, A. Bioinorganic photochemistry: Frontiers and mechanisms. *Chem Rev.* **2005**, *105*, 6: 2647-94. https://doi.org/10.1021/cr030707e

5. Brancaleon L, Moseley H. Laser and non-laser light sources for photodynamic therapy. *Lasers Med Sci*. **2002**, *17*, 3: 173-86. doi: 10.1007/s101030200027.

6. Castano AP, Demidova TN, Hamblin MR. Mechanisms in photodynamic therapy: Part three-Photosensitizer pharmacokinetics, biodistribution, tumor localization and modes of tumor destruction. *Photodiagnosis Photodyn Ther*. **2005**, *2*, 2: 91-106. doi: 10.1016/S1572-1000(05)00060-8.

7. Josefsen LB, Boyle RW. Photodynamic therapy and the development of metal-based photosensitisers. *Met Based Drugs*. **2008**, *2008*. https://doi.org/10.1155/2008/276109
8. Yoon HY, Cheon YK, Choi HJ, Shim CS. Role of photodynamic therapy in the palliation of obstructing esophageal cancer. *Korean J Intern Med*. **2012**, *27,* 3: 278-84. https://doi.org/10.3904/kjim.2012.27.3.278

9. Argiris A, Karamouzis MV, Raben D, Ferris RL. Head and neck cancer. *Lancet*. **2008** , *371*, 9625: 1695-709. https://doi.org/10.1016/s0140-6736(08)60728-x

10. Dilkes MG, DeJode ML, Gardiner Q, Kenyon GS, McKelvie P. Treatment of head and neck cancer with photodynamic therapy: results after one year. *J Laryngol Otol*. **1995,** *109*, 11: 1072-6. https://doi.org/10.1017/S0022215100132050

11. Mirzaei H, Djavid GE, Hadizadeh M, Jahanshiri-Moghadam M, Hajian P. The efficacy of Radachlorin-mediated photodynamic therapy in human hepatocellular carcinoma cells. *J Photochem Photobiol B*. **2015**, *142*: 86-91. https://doi.org/10.1016/j.jphotobiol.2014.11.007.

12. Battersby AR. Tetrapyrroles: the pigments of life. *Nat Prod Rep*. **2000**, *17*, 6 :507-26. https://doi.org/10.1039/b002635m.

13. De Freitas, L. F., & Hamblin, M. R. Antimicrobial photoinactivation with functionalized fullerenes. Elsevier eBooks, **2016.** https://doi.org/10.1016/B978-0-323-42864-4.00001-4

14. Allison RR, Sibata CH. Oncologic photodynamic therapy photosensitizers: a clinical review. *Photodiagnosis Photodyn Ther*. **2010**, *7*, 2: 61-75. https://doi.org/10.1016/j.pdpdt.2010.02.001

15. Abrahamse H, Hamblin MR. New photosensitizers for photodynamic therapy. *Biochem J*. **2016**, *473*, 4: 347-64. https://doi.org/10.1042/BJ20150942.

16. Krammer B, Plaetzer K. ALA and its clinical impact, from bench to bedside. *Photochem Photobiol Sci*. **2008**, *7*, 3: 283-9. https://doi.org/10.1039/b712847a.

17. Pignatelli P, Umme S, D'Antonio DL, Piattelli A, Curia MC. Reactive Oxygen Species Produced by 5-Aminolevulinic Acid Photodynamic Therapy in the Treatment of Cancer. *Int J Mol Sci*. **2023,** *24*, 10: 8964. https://doi.org/10.3390/ijms24108964.

18. Szeimies RM, Morton CA, Sidoroff A, Braathen LR. Photodynamic therapy for non-melanoma skin cancer. *Acta Derm Venereol*. **2005**, *85*, 6: 483-90. https://doi.org/10.1080/00015550510044136.

19. Irwin A.P. Linares, Leticia P. Martinelli, Milene N.O. Moritz, Heloisa S. Selistre-de-Araujo, Kleber T. de Oliveira, Janice Rodrigues Perussi,
Cytotoxicity of structurally-modified chlorins aimed for photodynamic therapy applications, *Journal of Photochemistry and Photobiology A: Chemistry*, 2022, 425, 113647. https://doi.org/10.1016/j.jphotochem.2021.113647.

20. Mroz P, Szokalska A, Wu MX, Hamblin MR. Photodynamic therapy of tumors can lead to development of systemic antigen-specific immune response. *PLoS One*. **2010**, *5*, 12. https://doi.org/10.1371/journal.pone.0015194.

21. Usuda J, Kato H, Okunaka T, Furukawa K, Tsutsui H, Yamada K, Suga Y, Honda H, Nagatsuka Y, Ohira T, Tsuboi M, Hirano T. Photodynamic therapy (PDT) for lung cancers. *J Thorac Oncol*. **2006**, *1*, 5: 489-93.

22. Lorenz KJ, Maier H. Plattenepithelkarzinome im Kopf-Hals-Bereich. Photodynamische Therapie mit Foscan [Squamous cell carcinoma of the head and neck. Photodynamic therapy with Foscan]. *HNO*. **2008**, *56*, 4: 402-9. https://doi.org/10.1007/s00106-007-1573-1.

23. Azzouzi AR, Lebdai S, Benzaghou F, Stief C. Vascular-targeted photodynamic therapy with TOOKAD® Soluble in localized prostate cancer: standardization of the procedure. *World J Urol*. **2015**, *33*, 7: 937-44. https://doi.org/10.1007/s00345-015-1535-2.
24. Mroz P, Huang YY, Szokalska A, Zhiyentayev T, Janjua S, Nifli AP, Sherwood ME, Ruzié C, Borbas KE, Fan D, Krayer M, Balasubramanian T, Yang E, Kee HL, Kirmaier C, Diers JR, Bocian DF, Holten D, Lindsey JS, Hamblin MR. Stable synthetic bacteriochlorins overcome the resistance of melanoma to photodynamic therapy. *FASEB J*. **2010**, *24*, 9: 3160-70. https://doi.org/10.1096/fj.09-152587.

25. Huang YY, Balasubramanian T, Yang E, Luo D, Diers JR, Bocian DF, Lindsey JS, Holten D, Hamblin MR. Stable synthetic bacteriochlorins for photodynamic therapy: role of dicyano peripheral groups, central metal substitution (2H, Zn, Pd), and Cremophor EL delivery. *ChemMedChem*. **2012**, *7*, 12: 2155-67. https://doi.org/10.1002/cmdc.201200351.

26. Roguin LP, Chiarante N, García Vior MC, Marino J. Zinc(II) phthalocyanines as photosensitizers for antitumor photodynamic therapy. *Int J Biochem Cell Biol*. **2019,** *114*: 105575. https://doi.org/10.1016/j.biocel.2019.105575.

27. Bing-De Zheng, Qin-Xue He, Xingshu Li, Juyoung Yoon, Jian-Dong Huang. Phthalocyanines as contrast agents for photothermal therapy, *Coordination Chemistry Reviews,* **2021**, *426*,https://doi.org/10.1016/j.ccr.2020.213548.

28. Davood Ajloo, Seyyed Morteza Fazeli, Farhad Janbaz Amirani. Interaction of Cationic and Anionic Phthalocyanines with Adenosine Deaminase, Molecular Dynamics Simulation and Docking Studies. *Computational Molecular Bioscience*. **2013**, *3*, 4, http://dx.doi.org/10.4236/cmb.2013.34010

29. Portolés, Francisco Garnes. Nuevas reacciones de acoplamiento cruzado de alquenos terminales altamente regioselectivas y catalizadas por paladio. *Universitat Politècnica de València*, **2023**.

30. Kollar J, Machacek M, Halaskova M, Lenco J, Kucera R, Demuth J, Rohlickova M, Hasonova K, Miletin M, Novakova V, Zimcik P. Cationic Versus Anionic Phthalocyanines for Photodynamic Therapy: What a Difference the Charge Makes. *J Med Chem*. **2020**, *63*, 14: 7616-7632. https://doi.org/10.1021/acs.jmedchem.0c00481.

31. Sumitomo Bakelite Co. Aromatic carboxylic acids, acid halides thereof and processes for preparing both. *United States patent.* **2003**.

32. Xiang S,Liao T,Zhao D,et al. A new multidentate hexacarboxylic acid for the construction of porous metal-organic frameworks of diverse structures and porosities. *Crystal Growth & Design*. **2010**, *10*, 6: 2775-2779.

33. JSME. Molecular Drawing Tool. Universidad de Alcalá. https://biomodel.uah.es/.
34. Miyaura, N. and Suzuki. Palladium-Catalyzed Cross-Coupling Reactions of Organoboron Compounds. *Chem. Rev*. **1995**, *95*, 7: 2457–2483. https://doi.org/10.1021/cr00039a007.

35. Krammer B, Plaetzer K. ALA and its clinical impact, from bench to bedside. *Photochem Photobiol Sci*. **2008**, *7*, 3: 283-9. https://doi.org/10.1039/b712847a.
36. Chan WM, Lim TH, Pece A, Silva R, Yoshimura N. Verteporfin PDT for non-standard indications--a review of current literature. *Graefes Arch Clin Exp Ophthalmol*. **2010**, *248*, 5: 613-26. https://doi.org/10.1007/s00417-010-1307-z.

37. Li, X., et al. Phthalocyanines as medicinal photosensitizers: Developments in the last five years. *Coordination Chemistry Reviews*. **2019**, *379*: 147-160. https://doi.org/10.1016/j.ccr.2017.08.003.

38. Carey, F.A. Química Orgánica, 9th edition. Madrid : *McGraw-Hill*, **2014.**

39. Klein, D. Quimica organica. Madrid : *Editorial Médica Panamericana*, **2014.**

40. N. Miyaura and A. Suzuki. *Chem. Rev*. **1995**, *95*, 2457.

41. Yin J, Rainka MP, Zhang XX, Buchwald SL. A highly active Suzuki catalyst for the synthesis of sterically hindered biaryls: novel ligand coordination. *J Am Chem Soc*. **2002**, *124*, 7: 1162-3. https://doi.org/10.1021/ja017082r.

42. Eu S, Katoh T, Umeyama T, Matano Y, Imahori H. Synthesis of sterically hindered phthalocyanines and their applications to dye-sensitized solar cells. *Dalton Trans*. **2008** *40*: 5476-83. https://doi.org/10.1039/b803272f.

43. Liu W, Jensen TJ, Fronczek FR, Hammer RP, Smith KM, Vicente MG. Synthesis and cellular studies of nonaggregated water-soluble phthalocyanines. *J Med Chem*. **2005**, *48*, 4: 1033-41. https://doi.org/10.1021/jm049375b.

44. Fernández-Guarino, M., García-Morales, I., Harto, A., Montull, C., Pérez- García, B., & Jaén. Terapia fotodinámica: nuevas indicaciones. *Actas Dermo-Sifiliográficas*. **2007**, *98*, 6: 377-395.

45. Dougherty TJ. Hematoporphyrin derivative for detection and treatment of cancer. *J Surg Oncol*. **1980**, *15*, 3: 209-10. https://doi.org/10.1002/jso.2930150303.

46. A. F. Littke, C. Dai and G. C. Fu. Versatile Catalysts for the Suzuki Cross-Coupling of Arylboronic Acids with Aryl and Vinyl Halides and Triflates under Mild Conditions. *Am. Chem. Soc*, **2000**, *122*, 4020. http://dx.doi.org/10.1021/ja0002058